

Helix Orientation of the Functional Domains in Apolipoprotein E in Discoidal High Density Lipoprotein Particles*

Received for publication, December 5, 2003, and in revised form, January 21, 2004
Published, JBC Papers in Press, January 21, 2004, DOI 10.1074/jbc.M313318200

Vasanthi Narayanaswami[‡], J. Nicholas Maiorano[§], Padmaja Dhanasekaran[¶], Robert O. Ryan[‡],
Michael C. Phillips[¶], Sissel Lund-Katz[¶], and W. Sean Davidson[§]

From the [‡]Lipid Biology in Health and Disease Research Group, Children's Hospital Oakland Research Institute, Oakland, California 94609, the [§]Department of Pathology and Laboratory Medicine, University of Cincinnati, Cincinnati, Ohio 45267, and [¶]Children's Hospital of Philadelphia, University of Pennsylvania School of Medicine, Philadelphia, Pennsylvania 19104-4318

Human apolipoprotein E (apoE) mediates high affinity binding to the low density lipoprotein receptor when present on a lipidated complex. In the absence of lipid, however, apoE does not bind the receptor. Whereas the x-ray structure of lipid-free apoE3 N-terminal (NT) domain is known, the structural organization of its lipid-associated, receptor-active conformation is poorly understood. To study the organization of apoE amphipathic α -helices in a lipid-associated state, single tryptophan-containing apoE3 variants were employed in fluorescence quenching studies. The relative positions of the Trp residues with respect to the phospholipid component of apoE/lipid particles were established from the degree of quenching by phospholipids bearing nitroxide groups at various positions along their fatty acyl chains. Four apoE3-NT variants bearing Trp reporter groups at positions 141, 148, 155, or 162 within helix 4 and two apoE3 variants containing single Trp at positions 257 or 264 in the C-terminal (CT) domain, were reconstituted into phospholipid-containing discoidal complexes. Parallax analysis revealed that each engineered Trp residue in helix 4 of apoE3-NT, as well as those in the CT domain of apoE, localized ~ 5 Å from the center of the bilayer. Circular dichroism studies revealed that lipid association induces additional helix formation in apoE. Protease protection assays suggest the flexible loop segment between the NT and CT domains may transition from unstructured to helix upon lipid association. Taken together, these data support a model wherein the α -helices in the receptor-binding region and the CT domain of apoE align perpendicular to the fatty acyl chains of the phospholipid bilayer. In this alignment, the residues of helix 4 are arrayed in a positively charged, curved helical segment for optimal receptor interaction.

Apolipoprotein E (ApoE) is a key regulator of plasma cholesterol homeostasis. Its interactions with the low density lipoprotein receptor (LDLR)¹ family and cell surface heparan sulfate

proteoglycans (1–3) are a critical step for the cellular uptake of apoE-containing lipoproteins. Transgenic mice overexpressing apoE manifest decreased plasma cholesterol levels on chow diet and a marked resistance to hypercholesterolemia on a high cholesterol/fat diet (4). On the other hand, apoE-deficient subjects display features of type III hyperlipoproteinemia (5) and apoE null mice exhibit massive accumulation of remnant lipoproteins (6), documenting the direct relevance of apoE in lipoprotein metabolism. However, structural features of lipid-associated apoE responsible for its receptor interaction properties are not understood at the molecular level.

ApoE comprises two independently folded structural and functional domains that are linked by a protease-sensitive loop segment. The globular 22 kDa N-terminal (NT) domain houses the LDLR recognition site, whereas the 10 kDa C-terminal (CT) domain bears high affinity lipoprotein-binding and self-association sites (7, 8). The NT domain is composed of four elongated amphipathic α -helices organized as an up-and-down helix bundle in the absence of lipid (9, 10). Helix 4 of the NT domain (residues 131–164) harbors key residues required for interaction with lipoprotein receptors (1). However, lipid association is a requirement for apoE (full-length or NT domain) to display receptor recognition capability, with apoE bound to model lipid particles displaying receptor binding ability comparable with that of native apoE-containing lipoproteins (11). Upon interaction with lipid it has been proposed that the NT domain helix bundle “opens” to expose the hydrophobic faces of its amphipathic helices to potential lipid surface binding sites, thereby achieving a receptor-active conformation (1, 12). Monolayer surface balance studies at the air/water interface provide evidence that the NT domain occupies a larger surface area than can be accounted for by its globular 4-helix bundle conformation (13), consistent with adoption of an “open” conformation. Subsequent fluorescence energy transfer analysis revealed that helical segments in the NT domain realign as a function of the transition from lipid-free helix bundle to lipid-bound state (12, 14). Attenuated total reflectance Fourier-transformed infrared spectroscopic studies (15) indicate that apoE-NT α -helices orient perpendicular to phospholipid (PL) acyl chains in discoidal complexes, although another report indicates a parallel orientation (16). Recent NMR spectroscopy studies provided evidence for increased solvent exposure of positively charged

* This work was supported by National Institutes of Health Grants HL56083 (to S. L.-K.), HL67093 (to W. S. D.), and HL64159 (to R. O. R.) and a Pfizer International HDL Research Award (to V. N.). The costs of publication of this article were defrayed in part by the payment of page charges. This article must therefore be hereby marked “advertisement” in accordance with 18 U.S.C. Section 1734 solely to indicate this fact.

¶ To whom correspondence should be addressed: Joseph Stokes Jr. Research Institute, The Children's Hospital of Philadelphia, Abramson Bldg., 3516 Civic Center Blvd., Philadelphia, PA 19104-4318. E-mail: Katzs@email.chop.edu.

¹ The abbreviations used are: LDLR, low density lipoprotein receptor;

apoE, apolipoprotein E; HDL, high density lipoprotein; rHDL, reconstituted HDL; DMPC, dimyristoylphosphatidylcholine; PL, phospholipid; POPC, 1-palmitoyl-2-oleoylphosphatidylcholine; PSFC, 1-palmitoyl-2-stearoyl-phosphatidylcholine; λ_{\max} , wavelength of maximum fluorescence.

amino acid side chains in the receptor-binding region upon interaction of the NT domain with lipid (17).

With regard to the CT domain, the precise molecular features responsible for high affinity lipid binding are not known, although it is believed that CT domain interaction with lipids is mediated by putative amphipathic α -helices (1). Using deletion mutagenesis, Westerlund and Weisgraber (18) demonstrated that residues 267–299 contribute to the lipoprotein binding properties of apoE. In other studies, Dong *et al.* (19) reported that residues 260–272 are important for complete lipoprotein association.

To address questions relating to the alignment and orientation of the receptor-binding region of the NT domain and lipid-binding sites in the CT domain of lipid-associated apoE, we examined the relative ability of spatially defined nitroxide-labeled PL to quench the fluorescence of a panel of unique single Trp apoE3 variants in reconstituted high density lipoproteins (rHDL). It was determined that the engineered Trp residues in helix 4 align uniformly, close to the center of the PL bilayer, thereby presenting the receptor-binding site as a positively charged, curved helical segment analogous to that displayed on spherical lipoprotein particles.

EXPERIMENTAL PROCEDURES

Materials—1-Palmitoyl-2-oleoylphosphatidylcholine (POPC) and the nitroxide spin probes 1-palmitoyl-2-stearoyl-(X-DOXYL)-sn-glycero-3-phosphocholine (where X = 5, 7, 10, 12, or 16) and dimyristoylphosphatidylcholine (DMPC) were purchased from Avanti Polar Lipids (Birmingham, AL). The single Trp synthetic peptides K₂WL₉AL₉K₂A and K₂GL₉WL₉K₂A were a generous gift of Dr. Erwin London at the State University of New York at Stony Brook. Human thrombin was obtained from Hematologic Technologies Inc. All other reagents were analytical grade.

Site-directed Mutagenesis, Protein Expression, and Purification—Single Trp mutants were introduced in a Trp null apoE3-NT (residues 1–183) variant by site directed-mutagenesis and expressed in *Escherichia coli* as described (14, 20). Full-length apoE3 bearing single Trp residues at position 257 or 264 were constructed using the QuikChange® mutagenesis protocol (Stratagene, La Jolla, CA) in a strategy similar to that described elsewhere (14). All constructs were verified by restriction analysis and double-stranded DNA sequencing in both directions. Single Trp-containing apoE3 variants were expressed and purified as thioredoxin fusion proteins in *E. coli* upon subcloning into a pET32a(+) vector (17, 21) following manipulations to optimize codon usage for bacterial expression (22). Intact apoE preparations without the GST fusion protein were at least 95% pure as assessed by SDS-PAGE.

Preparation and Characterization of rHDL—ApoE3 variants (2–3 mg/ml) were dissolved in 100 mM ammonium bicarbonate, pH 8.0, containing 6 M guanidine HCl and 5 μ l of β -mercaptoethanol/mg of protein. The solutions were dialyzed against 100 mM ammonium bicarbonate, pH 8.0. rHDL were prepared as described previously (23) using POPC, a specified apoE3 variant, a given DOXYL-PL, and sodium cholate, except that the lipids were subjected to bath sonication for 30 min prior to addition of sodium cholate. The DOXYL moieties were located at positions C-5, C-7, C-10, C-12, or C-16 along the stearoyl chain of POPC at the sn-2 position. Initial PL:DOXYL-PL:apoE molar ratios were 49:9:1. For each apoE3 variant, particles were reconstituted with and without DOXYL-PL to characterize the Trp fluorescence contribution in the presence and the absence of quencher, respectively. In rHDL lacking DOXYL-PL, the corresponding PL mass was replaced by POPC to maintain uniformity in particle lipid to protein ratio. The rHDL were isolated by gel filtration chromatography on a Superdex 200 gel filtration column (24) to remove unbound protein and/or vesicular structures. Particle hydrodynamic properties were assessed by gradient native polyacrylamide electrophoresis and/or Superdex 200 gel filtration chromatography (24).

Fluorescence Spectroscopy—Fluorescence measurements were performed on a Photon Technology International Quantamaster spectrometer in photon counting mode. For each variant, an aliquot of the rHDL samples, with or without quenchers, was diluted in buffer. Fluorescence emission spectra were recorded from 303 to 375 nm at an excitation wavelength of 295 nm in order to minimize the contribution of tyrosine fluorescence in apoE. Emission and excitation band-passes were 3.0

nm. Fluorescence analysis was carried out at 25 °C in a semi-micro-quartz cuvette. The spectra were corrected for background fluorescence of buffer alone. The spectra were not corrected for the spectral characteristics of the emission and excitation monochromators.

Trp Depth Calculations—The parallax method for determining the depth of penetration of a fluorophore in a lipid bilayer was derived by Chattopadhyay and London (25) from conventional relationships of static quenchers to randomly distributed fluorophores. The differences in fluorescence intensities of the fluorophore in the presence of known concentrations of nitroxide quencher groups at known locations in a PL acyl chain are used to calculate the depth of the fluorophore relative to the quenchers (see Ref. 23 for a detailed discussion of the method theory). The distance of the Trp from the center of the bilayer (Z_{cf}) is given by

$$Z_{cf} = L_{cs} + [-\ln(F_s/F_d)/\pi C - L_{ds}^2]/2L_{ds} \quad (\text{Eq. 1})$$

where F_s is the fluorescence intensity in the presence of the shallow quencher, F_d is the same for the deep quencher, L_{cs} is the distance from the center of the bilayer to the shallow quencher, L_{ds} is the distance between the shallow and deep quenchers, and C is the concentration of the quencher molecules per \AA^2 . Equation 1 is valid when nitroxide groups that are shallow in the membrane quench the Trp residue. When the Trp is buried deep within the membrane, however, it is subjected to quenching from groups in the opposite leaflet the lipid bilayer. For this situation, a second relationship is required to account for trans-bilayer quenching,

$$Z_{cf} = L_{cd} - [\ln((F_s/F_o)^2/(F_d/F_o))/\pi C) - 2L_{ds}^2 + 4L_{cd}^2]/4(L_{ds} + L_{cd}) \quad (\text{Eq. 2})$$

where F_o is the fluorescence intensity in the absence of quencher, L_{cd} is the distance from the center of the bilayer to the deep quencher, and L_{ds} is the distance between the shallow and deep quenchers. Equation 2 was used in this study whenever a Trp residue was determined to be <6 \AA from the center of the membrane by Equation 1.

Circular Dichroism Spectroscopy—Circular dichroism (CD) spectra were collected on a Jasco J600 or J720 spectropolarimeter equipped with a temperature-controlling device and interfaced with a computer. The molar ellipticity ($[\theta]$) in degrees $\text{cm}^2 \text{dmol}^{-1}$ at 222 or 208 nm was calculated from the equation $[\theta] = (\text{MRW} \cdot \theta)/(10d \cdot c)$, where MRW is the mean residue weight of the apoE CT domain calculated to be 114.31, θ is the measured ellipticity in degrees at 222 or 208 nm, d is the cuvette path length in cm, and c is the protein concentration in g/ml. The α -helical content of each rHDL preparation was derived from the molar ellipticity at 222 nm by established procedures (26, 27). In other analyses, lipid-free apoE3 was incubated overnight in the absence or in the presence of trifluoroethanol (50% v/v) prior to CD analysis. In addition, spectra of apoE3-DMPC complexes were obtained (28).

Thrombin Digestion—The effect of lipid association on accessibility to thrombin digestion was examined by treating 20 μ g of apoE3 in a lipid-free or DMPC-bound state (14) in 20 mM Tris-HCl, pH 8.5, 150 mM NaCl, 2.5 mM CaCl₂ with 1 milliunit of thrombin for 3 h at 37 °C. The samples were analyzed on a 4–20% acrylamide gradient by SDS-PAGE with untreated lipid-free or -bound apoE3 as control.

Analytical Procedures—Protein concentrations were determined by the Lowry procedure (29) or by A₂₈₀ measurements using an extinction coefficient of 1.34 for 1 mg of full-length apoE3 protein/ml or 1.32 for 1 mg of apoE3 NT domain protein/ml. PL content was determined by phosphorus analysis (30).

RESULTS

Experimental Strategy—Receptor binding analyses of genetically engineered and naturally occurring variants of apoE have demonstrated that residues in the region of residues 134–150 of apoE3 are indispensable for receptor binding activity (1). High resolution structural information on lipid-free human apoE3-(1–191) reveals that helix 4 spans residues 131–164 (9), thereby encompassing the entire receptor-binding element. Using a variety of biophysical approaches, it has been shown that the NT domain helix bundle undergoes a conformational change upon interaction with lipid (see Ref. 31 for a review). Whereas the precise structural alteration that accompanies lipid association of the NT domain is not known, this conformational adaptation confers the protein with LDLR-rec

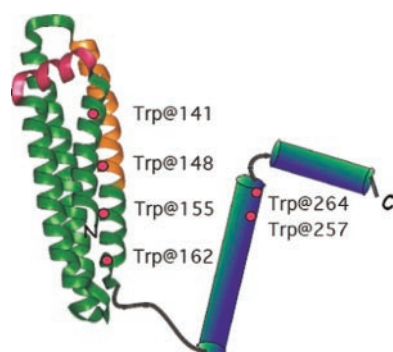


FIG. 1. **Model structure of apoE3.** The NT domain is shown as a ribbon diagram with the four amphipathic α -helices depicted in green (9). The CT domain is modeled as amphipathic helices based on Segrest *et al.* (39) and Choy *et al.* (47). The receptor-binding segment on helix 4 is indicated in gold, and the short helix that links helices 1 and 2 is shown in pink. Filled circles represent the sites where single Trp residues were introduced into an NT domain construct, and single Trp residues introduced into the CT domain of full-length apoE3.

ognition properties (32). Because the lipid-bound apoE3-NT mimics full-length apoE3 in terms of receptor binding activity, we used this domain in studies designed to characterize the orientation and positioning of helix 4 in lipid-associated apoE3-NT. Isolated recombinant apoE3-NT domain was reconstituted with PL to generate a homogeneous population of discoidal lipid particles that are known to be LDLR-active (32). To evaluate the disposition of the receptor-interaction site with respect to the lipid surface, a series of apoE3-NT domain variants possessing a single Trp residue positioned along the length of helix 4 (at positions 141, 148, 155, or 162; see Fig. 1) were subjected to fluorescence spectroscopy. By examining the relative ability of a series of DOXYL-PL (with the nitroxide moiety located at different positions along the fatty acyl chain) to quench apoE3-NT Trp fluorescence, the relative position of the Trp probes with respect to PL bilayer can be deduced. For example, if helix 4 retains its general organization and aligns with its helical axis parallel to the PL acyl chains, large differences in nitroxide quenching behavior would be anticipated for the different single Trp variants positioned at every second turn of the helix. On the other hand, if helix 4 aligns perpendicular to the PL acyl chains, the extent of nitroxide quenching will be similar for each of the single Trp variants.

Characterization of apoE3 Variant Lipid Particles—Reconstituted lipid particles composed of POPC, a given DOXYL-PL, and a unique single Trp apoE3 variant, were found to be of uniform size as judged by native gradient PAGE analysis. In each case the particles displayed an average diameter of 115 ± 10 Å, consistent with findings reported for wild type apoE3-NT domain (20). No differences were observed in the physical characteristics of complexes prepared with POPC alone versus POPC plus DOXYL-PL. A similar lack of a structural perturbation from the DOXYL-PL was previously noted for particles made with apoA-I (23, 33). Taken together, these data indicate that the apoE3 variants employed in this study retained their lipid binding ability and that incorporation of DOXYL-PL in the reconstituted particles did not significantly alter their size or hydrodynamic properties. Furthermore, far UV circular dichroism analysis of a subset of the disc particles employed in this study consistently yielded 70–75% α -helix content.

Trp Fluorescence Studies—Prior to analysis of the Trp quenching patterns in rHDL containing the different single Trp apoE3 variants, control experiments were performed to validate the quenching protocol and to ensure that the nitroxide moieties quench at the expected depth under the conditions employed to reconstitute apoE3 into lipid particles. Two hydro-

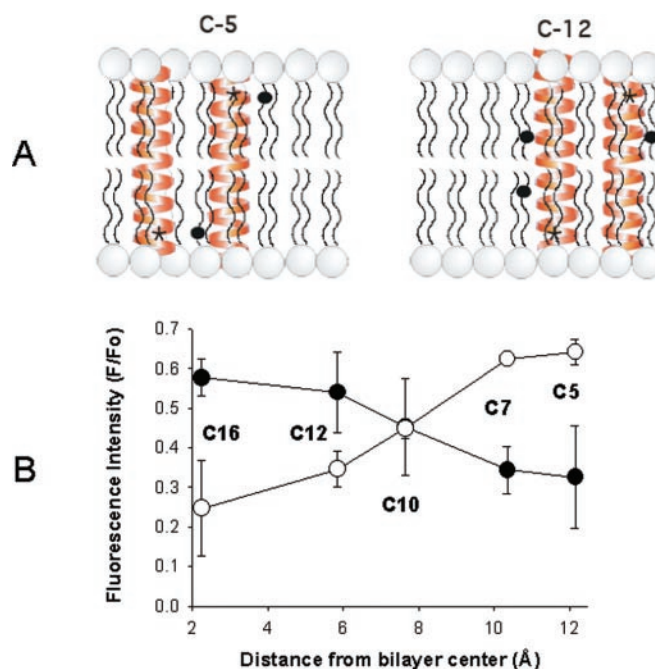


FIG. 2. **Nitroxide lipid quenching of single Trp-containing, transmembrane peptides in small unilamellar vesicles.** A, schematic representation of the positioning of PL DOXYL moieties (black circles) with respect to a model transmembrane helix. The situation for both the shallowest (C-5, left) and deepest (C-12, right) DOXYL moieties are shown. The asterisk indicates the shallow Trp in peptide 1 ($K_2WL_9AL_9K_2A$). B, small unilamellar vesicles containing peptide 1 ($K_2WL_9AL_9K_2A$ (filled circles)) or peptide 2 ($K_2GL_9WL_9K_2A$ (open circles)) and X-DOXYL-PL (where X = carbon position 2, 6, 8, 10, or 12 on the fatty acyl chain) were prepared as described under "Experimental Procedures." The molar ratio of POPC:X-DOXYL-PL:peptide was 65:12:1. Emission spectra were recorded between 303 and 375 nm (excitation wavelength of 295 nm), and F/F_0 was plotted as a function of the calculated distance of the various DOXYL groups on the fatty acyl chains from the center of the bilayer (34).

phobic α -helical peptides that possess a single Trp residue at different points along the length of the helix were employed. Ren *et al.* (34) have previously demonstrated that these peptides traverse the membrane of small unilamellar vesicles and orient parallel to the acyl chains. Peptide 1 ($K_2WL_9AL_9K_2A$) contains a membrane-spanning sequence composed primarily of repeating leucines flanked by pairs of lysine residues. The Trp in peptide 1 is located near one end of the helix. Peptide 2 ($K_2GL_9WL_9K_2A$) is similar in design but contains a Trp at the center of the peptide sequence. Hence, when inserted into a membrane the Trp in peptide 1 is expected to locate close to the polar/apolar interface, as depicted in Fig. 2A, whereas peptide 2 is expected to be located near the center of the bilayer. Reconstitution of peptides 1 and 2 into vesicles containing specific DOXYL-PL and fluorescence analysis revealed that the Trp in $K_2WL_9AL_9K_2A$ was maximally quenched when the DOXYL moiety was located at position C-5, 12 Å from the bilayer center (Fig. 2B). The extent of quenching observed decreased as the DOXYL moiety was positioned further down the acyl chain. Peptide 2 exhibited the opposite quenching pattern, wherein Trp fluorescence was minimally quenched when the DOXYL moiety was located at C-5 and was maximally quenched by C-16 DOXYL-PL (2 Å from the bilayer center). The calculated depths of these Trp residues were 15.4 ± 2.2 Å for peptide 1 and 3.0 ± 2.6 Å from the bilayer center for peptide 2.

ApoE3 NT rHDL—The wavelength of maximal fluorescence emission intensity (λ_{max}) for each single Trp apoE3 variant (excitation 295 nm) was determined in the absence of nitroxide

TABLE I
Fluorescence characteristics and parallax analysis of single Trp apoE3 variants in rHDL particles

ApoE3 variant	λ_{\max}^a	Z_{ct}^b
	nm	Å
NT domain		
Trp-141	330.0 ^c	4.4 ^c
Trp-148	332.0 ^c	5.7 ^c
Trp-155	330.7 ± 1.2	4.9 ± 0.3 ^d
Trp-162	332.0 ± 1.0	4.7 ± 0.2 ^e
CT domain		
Trp-257	332.0 ± 0.0	4.7 ± 0.6 ^e
Trp-264	332.3 ± 0.6	5.2 ± 0.6 ^d

^a Wavelength of maximum fluorescence.

^b Depth of penetration of the Trp residue measured from the bilayer center (0 Å); calculated from Equations 1 and 2 under "Experimental Procedures."

^c Because of poor recovery from the gel filtration column, these samples were measured in duplicate. Values shown are the average of two measurements.

^d $n = 3$.

^e $n = 4$.

labeled PL (Table I). In each case reconstitution of the single Trp variant apoE3 NT variant with POPC resulted in a λ_{\max} value of ~330–332 nm. Considering that solvent-exposed Trp residues exhibit λ_{\max} values in the range of 350 nm, this result indicates that these Trp residues are not exposed to the aqueous environment and, therefore, are well suited for lipid-based quenching studies. We then determined the effect of specific DOXYL-PL on the fluorescence intensity of lipid associated single Trp apoE3-NT variants. Data are shown as a plot of F/F_0 (where F and F_0 represent fluorescence intensities in the presence and absence of quencher, respectively) versus DOXYL moiety distance from the PL bilayer center. In the case of Trp-141 apoE3-NT, the DOXYL-PL with the quencher located at position C-5 of the fatty acyl chain (12 Å from bilayer center), was the least effective (Fig. 3, top panel). As the DOXYL moiety was positioned further along the fatty acyl chain (*i.e.* deeper into the membrane), Trp-141 fluorescence was increasingly quenched, with maximal quenching observed with quencher located at the C-12 position and decreasing at C-16. ApoE3-NT variants with Trp at position 148 or 162 displayed a similar pattern of quenching. In the case of Trp-155 apoE3 NT domain, we confined our study to lipid particles possessing DOXYL moieties at positions C-5 and C-12 because of sample limitations. Despite this, we were able to calculate a reliable depth of penetration for this variant (see below). To determine the precise location of the Trp residues with respect to the bilayer, the distance of each Trp from the center of the bilayer was calculated using parallax analysis (25). This method uses the quenching ratio from a pair of quenchers, one shallow and one deep in the membrane (see "Experimental Procedures"). PL with DOXYL moieties at C-5 and C-12 were chosen for the calculation for two reasons: (i) this pair provides information close to the bilayer surface and relatively close to the bilayer center, respectively, and (ii) detailed information for the quenching of the two control peptides (employed in this study) and 7-nitro-2,1,3-benzoxadiazol-4-yl (NBD)-labeled phospholipid with quenchers located at positions C-5 and C-12 is available (35, 36). Table I summarizes the fluorescence characteristics and quenching data for the rHDL particles of the apoE3 variants. Each of the four single Trp apoE3-NT variants exhibited a narrow range of depth of location, between 4.4 and 5.7 Å, indicating that positions 141, 148, 155, and 162 along the hydrophobic face of helix 4 localize to similar depths in the PL bilayer.

The CT Domain of Full-length apoE—To examine the relative location of Trp-257 and Trp-264 in the CT domain of apoE3

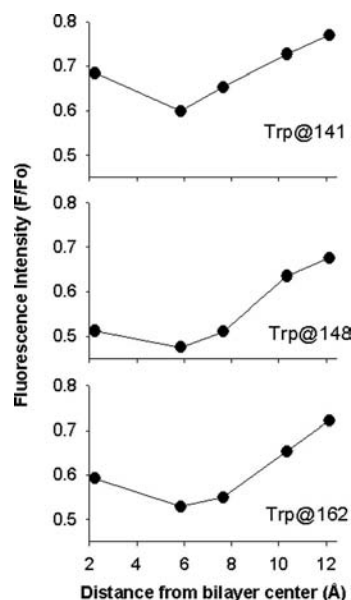


FIG. 3. Nitroxide lipid quenching of apoE3-NT single Trp mutants in rHDL particles. rHDL particles were prepared with Trp@141, Trp@148, or Trp@162/apoE3-NT at a molar ratio of 49:9:1 (POPC:DOXYL-PL:apoE3-NT variant) as described under "Experimental Procedures." The particles were separated from unreacted lipid vesicles and free protein by gel filtration chromatography, characterized, and used for fluorescence studies at concentrations of 50–100 μg of apoE/ml. F/F_0 is plotted as a function of DOXYL moiety distance from bilayer center. Each curve is a representative from a variable number of replicates (either three or six observations). The distance of each DOXYL group from the center of the membrane is as follows (in Å): C-5, 12.15; C-7, 10.35; C-10, 7.65; C-12, 5.85; and C-16, 2.25.

with respect to that of helix 4 of the NT domain, single Trp variants of full-length apoE3 were generated. The Trp residues were positioned at locations along the linear sequence of a predicted α -helix segment in the CT domain. Both single Trp apoE3 variants were incorporated into PL disc particles as described above for apoE3 NT. Fluorescence emission spectra of these apoE3 single Trp variants revealed blue-shifted λ_{\max} values similar to those observed for the NT domain (Table I). rHDL particles containing Trp-257 apoE3 or Trp-264 apoE3 with DOXYL-PL were subject to Trp fluorescence quenching analysis. Fig. 4 reveals that both Trps are maximally quenched by DOXYL moieties at C-12 position, corresponding to a distance of 4.7 and 5.2 Å, respectively, from the bilayer center (Table I). A comparison of this data with that obtained for single Trp variants within helix 4 of the NT domain indicates a similar orientation and alignment with respect to the lipid bilayer.

Secondary Structure of Intact apoE3 in the Presence of Trifluoroethanol or Lipid—We postulated that if intact apoE3 adopts a uniform orientation and alignment in complex with PL, it likely adopts an extended helical structure that propagates around the periphery of the disc-shaped bilayer, as proposed earlier (15). Such a rationale presupposes that apoE3 adopts increased helical structure in its lipid-bound state. Far UV CD spectroscopy was used to evaluate the secondary structure content of lipid-bound apoE3. The maximum helix forming potential of the protein was estimated by obtaining spectra of apoE3 in the presence of the helix inducing cosolvent, trifluoroethanol (37, 38). In buffer alone, apoE3 displays a high degree of α -helicity, as demonstrated by characteristic troughs at 222 and 208 nm with molar ellipticity values of $\sim 21,000^\circ \text{ cm}^2 \text{ dmol}^{-1}$ (about 62% helicity; Fig. 5). In the presence of trifluoroethanol (50% v/v), a 25% increase in molar ellipticity was noted at 222 nm. Insofar as lipid-associated apoE3 dis-

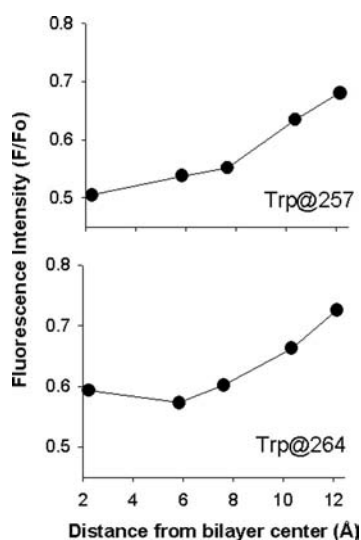


FIG. 4. Nitroxide lipid quenching of apoE3 single Trp mutants in rHDL particles. rHDL particles containing Trp@257/apoE3 or Trp@264/apoE3 at a molar ratio of 49:9:1 (POPC:DOXYL-PSPC:apoE3 variant) were prepared, and fluorescence measurements were carried out as described for Fig. 3.

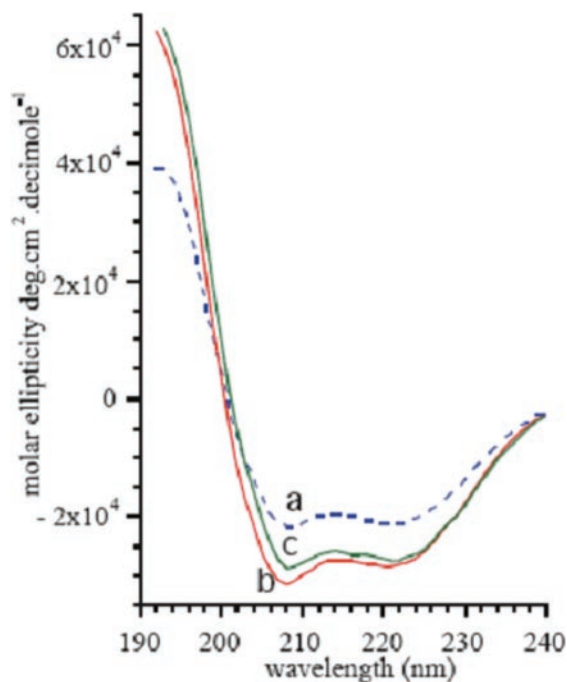


FIG. 5. Effect of trifluoroethanol and lipid on secondary structure characteristics of apoE3. Shown are far UV CD spectra of 2 mg/ml apoE3 in buffer alone (25 mM sodium phosphate, 50 mM NaCl, pH 7.5) (a), buffer plus 50% trifluoroethanol (v/v) (b), and apoE3 rHDL (c). CD measurements were carried out at 25 °C in an 0.02-cm path length cuvette.

played a similar increase in molar ellipticity, the data suggest that lipid interaction induces apoE to adopt nearly maximal helix content.

Effect of Thrombin Treatment—The NT domain of apoE3 is linked to the CT domain via a relatively unstructured, protease-sensitive segment spanning residues 191–210 (1). Earlier reports indicate that upon lipid interaction the sensitivity of apoE3 to proteases is lost (19). Under the conditions employed, we evaluated the accessibility of the loop segment to thrombin in lipid-free and lipid-bound apoE3 (Fig. 6). In the absence of lipid, thrombin digestion yielded two fragments, corresponding to the NT and CT domains, whereas apoE3 rHDL were resist-

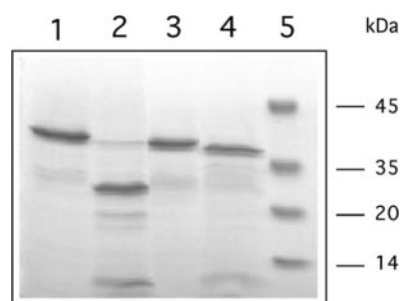


FIG. 6. Effect of thrombin on lipid-free and lipid-associated apoE3. ApoE3 (20 μ g) was incubated with 1 milliunit in 20 mM Tris-HCl, pH 8.5, 150 mM NaCl, 2.5 mM CaCl₂ at 37 °C for 3 h in a total volume of 20 μ l followed by the addition of SDS-PAGE sample treatment buffer and heating. The samples were then subjected to 4–20% SDS-PAGE. lane 1, apoE3; lane 2, apoE3 plus thrombin; lane 3, apoE3 rHDL; lane 4, apoE3 rHDL plus thrombin; lane 5, molecular mass standards.

ant to thrombin digestion. This observation is consistent with the CD analysis, suggesting that the observed increase in α -helicity may be because of lipid association-induced structuring of the loop segment to α -helix.

DISCUSSION

Lipid-based quenching experiments combined with parallax analysis have been used to define the positions of Trp residues in membrane-spanning proteins (40). More recently, this approach has been applied to the study of human apoA-I (23, 33). Parallax analysis revealed that all eight 22-amino acid helices within apoA-I were oriented perpendicular to the PL acyl chains in rHDL particles. In the present study, we employed the same methodology to evaluate two structural regions in apoE3, the lipoprotein receptor recognition site in the NT domain and a key lipid-binding region of the CT domain. The application of this methodology to apoE is appropriate because its primary sequence is dominated by amphipathic α -helices and the protein readily transforms PL vesicles into discoidal bilayer particles that manifest receptor-binding activity. Furthermore, the helix boundaries defined by the x-ray structure of apoE3-NT were useful for identifying mutagenesis sites within helix 4. The λ_{\max} values for the single Trp variants studied here are consistent with the Trps being buried in the lipid milieu and, therefore, amenable to quenching by DOXYL-PL incorporated into the rHDL particles.

We noted that optimal fluorescence quenching of the four unique single Trp apoE3-NT variants was achieved with PL bearing a DOXYL moiety at position C-12 of the fatty acyl chain. Furthermore, a consistent trend was observed with these variants wherein the extent of quenching decreased as a function of the distance away from the bilayer center the nitroxide label was positioned. Thus, with every apoE3 variant studied, the DOXYL-PL with a nitroxide moiety at C-5 was the poorest quencher. The consistent quenching behavior for these unique single Trp variants indicates that although the Trp residues are positioned across a span of 22 amino acids, they orient to a similar depth with respect to the PL fatty acyl chains. Considering that the residues examined in this study fall within the known boundaries of helix 4 of the apoE3 NT domain four-helix bundle, the data strongly suggest that this elongated α -helix segment is not interrupted upon lipid association and that the helix aligns around the perimeter of the disc complex, adopting an orientation that is perpendicular to the PL fatty acyl chains at an average of 5.0 Å from the center of the bilayer (Fig. 7). Clearly, if helix 4 aligned parallel to the fatty acyl chains (16), the Trp residues would be located at different depths along the helix and an entirely distinct quenching pattern would be observed.

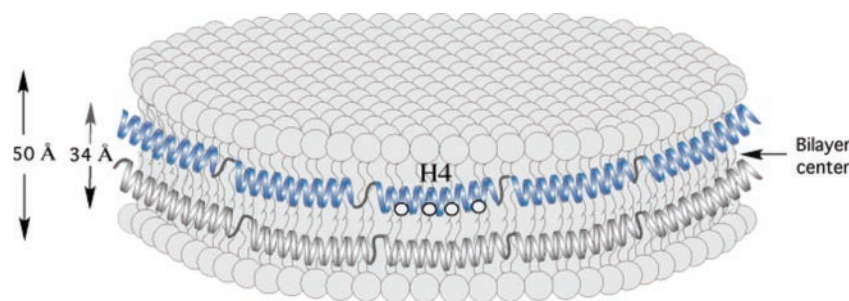


FIG. 7. **Putative model of apoE in rHDL depicting the location of Trp residues in the receptor-binding site.** The model represents the deep location of the engineered Trp moieties (circles) on helix 4, the LDL receptor-binding site on apoE. Two molecules of apoE (blue and gray) of a total of about 4 molecules/discoidal particle are depicted to circumscribe the periphery of a bilayer of phospholipids. The helical axes are orientated perpendicular to the phospholipid fatty acyl chains.

These data are particularly relevant to questions relating to the molecular basis of apoE interaction with LDLR family members. Whereas the x-ray crystal structure of apoE3-NT reveals that residues essential for interaction with the LDLR (*i.e.* 134–150) reside within helix 4 (9), it is also known that the lipid-free helix bundle conformation is not recognized by the receptor. The manifestation of receptor binding ability occurs upon lipid interaction, however, suggesting that either the relative exposure of residues within this region or the structural properties of this segment are altered upon lipid association. It is important to note that, in either DMPC or egg phosphatidylcholine (in which the primary molecular species is POPC) discoidal rHDL and spherical HDL, the affinities of apoE for the LDLR are essentially the same (11). By understanding the alignment and orientation of the receptor-binding element with respect to the lipid environment, we can begin to address the receptor-active conformation of apoE. Our data are consistent with a model wherein this region of the molecule aligns around the perimeter of disc shaped lipid particles. Given such an alignment and the curvature imposed by the geometry of the lipid particle, it is conceivable that manifestation of receptor recognition properties upon association with rHDL is related to increased exposure of charged amino acid side chains on the polar face of this amphipathic helix (17). Indeed it is plausible that curvature imposed on helix 4 by the geometry of the discoidal particle is generally analogous to that imposed by the surface curvature of spherical lipoproteins, perhaps explaining the manifestation of apoE LDLR recognition properties upon association with these distinct particles.

Another contributing factor may be an extension of helix 4 beyond the boundaries identified in the globular helix bundle conformation. Recent NMR studies of a 58-residue peptide that encompasses residues 126–183 suggest that lipid interaction leads to a structuring of residues between positions 165 and 179, amino acids that adopt random structure in the absence of lipid (41). Indeed, this hypothesis is consistent with the present helix alignment insofar as helix extension would not be precluded by disc particle geometry. Furthermore, such an extension would result in structuring of Arg-172 in a region of α -helix, providing a molecular explanation for the observation of Morrow *et al.* (42) that this residue is essential for optimal binding to the lipoprotein receptor.

The NT domain of apoE possesses all of the elements required for interaction with the LDLR; however, the 10-kDa CT domain also plays an important physiological role. Although structural information about this domain is limited, it is known to possess high lipid binding affinity and is responsible for apoE interaction with circulating lipoproteins (43). It has been hypothesized that tight association of the CT domain with the surface of circulating lipoproteins retains apoE at the particle surface, permitting the NT domain to transition between a

receptor-inactive helix bundle state and a receptor-active alternate conformation wherein key residues within this domain make contact with the lipid surface (31, 44). Although the NT and CT domains function in isolation and can be considered independent structural folds (7, 8), some degree of domain interaction appears to be responsible for the disparate lipoprotein binding properties of apoE3 *versus* apoE4 isoforms (19, 45, 46). Indeed, Glu-255 in the CT domain has been shown to form a salt bridge interaction with Arg-61 in apoE4, resulting in an altered lipoprotein binding preference for this isoform. Whether this interaction is maintained in lipid-associated apoE or is disrupted upon lipid binding is unknown. As a means of characterizing the nature of CT domain helix orientation and alignment on reconstituted lipid particles, we studied two single Trp apoE3 variants. Lipid-based nitroxide quenching experiments revealed that Trp residues at positions 257 and 264 localize to a similar depth position within the membrane. These residues were chosen to represent the lipoprotein-binding surface of apoE CT (18, 19), which is sequestered in an intermolecular helix-helix interaction in the lipid-free state (7, 37, 47, 48). The striking similarity in quenching behavior for Trp residues located in helix 4 of the NT domain and in distinct sites within the CT domain suggests that they adopt a similar alignment and orientation in rHDL. Further, CD analysis indicates that lipid association induces apoE3 to adopt increased α -helicity to the maximum possible limit set by trifluoroethanol interaction, suggesting loop segments and/or unstructured regions transition to helix. Whereas the linker loop connecting the NT and CT domains is unstructured and accessible to proteases in lipid-free state, lipid association renders this segment inaccessible to proteolysis, consistent with earlier observations (19); this result may be explained in part by transitioning to a helical structure. Taken together, these data raise the possibility that upon lipid association, apoE adopts an extended conformation wherein α -helical segments in the protein align in tandem around the perimeter of the disc in a belt-like manner.

If it is considered that the bilayer width for a liquid crystalline POPC bilayer is 50 Å, as measured by x-ray reflection techniques (15 mol % H₂O at 23 °C) (49), then 8 Å can be attributed to the polar head group regions of each leaflet (16 Å total) with the hydrophobic portion of the membrane comprising 34 Å. This gives two bilayer leaflets of about 17 Å that must be in contact with apolipoprotein to prevent unfavorable solvation of the acyl chains. If it is further considered that a given helix segment can interact stably with one leaflet, then a similar arrangement of a second apoE molecule on the adjacent leaflet may be envisaged (see Fig. 7). Because the Trp residues are located near the centerline of the hydrophobic region of the helices studied, there are 12 Å between the centers of the two helices. Assuming a typical apolipoprotein helical radius of

about 5.5 Å, the present fluorescence measurements are consistent with the edges of the α -helices in rHDL particles being clustered together at the center of the bilayer. It is conceivable that this arrangement is stabilized by the formation of interhelical salt bridges. We suggest that this structure (Fig. 7) projects the essential positively charged amino acids on the polar face of the helix as a cluster for optimal interaction with the LDLR.

It should be noted that the present study was confined to two specific regions of apoE that are predicted to exist as helices in the lipid bound state. Therefore, it could be that the remaining portions of the molecule exist in an alternate orientation. Evidence for such an alternate orientation was not found in detailed studies of apoA-I, wherein all helical segments were shown to exist in the same orientation (33). In fact, in all of our studies of helical domains within apoE or apoA-I, we have yet to identify a single Trp residue that is maximally quenched shallower than 6.6 Å from the bilayer center. Based on these observations, we propose that the perpendicular orientation of amphipathic helical domains with respect to PL acyl chains in disc particles is a common feature of amphipathic exchangeable apolipoproteins. Experiments with rHDL containing other members of the apolipoprotein family will be required to test this hypothesis.

Acknowledgment—We thank Dr. Cyril M. Kay, Department of Biochemistry, University of Alberta, Edmonton, Canada, for CD analysis of lipid-bound apoE3.

REFERENCES

- Weisgraber, K. H. (1994) *Adv. Protein Chem.* **45**, 249–302
- Mahley, R. W., and Huang, Y. (1999) *Curr. Opin. Lipidol.* **10**, 207–217
- Brown, M. S., and Goldstein, J. L. (1986) *Science* **232**, 34–47
- Shimano, H., Yamada, N., Katsuki, M., Yamamoto, K., Gotoda, T., Harada, K., Shimada, M., and Yazaki, Y. (1992) *J. Clin. Investig.* **90**, 2084–2091
- Schaefer, E. J., Gregg, R. E., Ghiselli, G., Forte, T. M., Ordovas, J. M., Zech, L. A., and Brewer, H. B., Jr. (1986) *J. Clin. Investig.* **78**, 1206–1219
- Zhang, S. H., Reddick, R. L., Piedrahita, J. A., and Maeda, N. (1992) *Science* **258**, 468–471
- Aggerbeck, L. P., Wetterau, J. R., Weisgraber, K. H., Wu, C. S., and Lindgren, F. T. (1988) *J. Biol. Chem.* **263**, 6249–6258
- Wetterau, J. R., Aggerbeck, L. P., Rall, S. C., Jr., and Weisgraber, K. H. (1988) *J. Biol. Chem.* **263**, 6240–6248
- Wilson, C., Wardell, M. R., Weisgraber, K. H., Mahley, R. W., and Agard, D. A. (1991) *Science* **252**, 1817–1822
- Segelke, B. W., Forstner, M., Knapp, M., Trakhanov, S. D., Parkin, S., Newhouse, Y. M., Bellamy, H. D., Weisgraber, K. H., and Rupp, B. (2000) *Protein Sci.* **9**, 886–897
- Innerarity, T. L., Pitas, R. E., and Mahley, R. W. (1979) *J. Biol. Chem.* **254**, 4186–4190
- Fisher, C. A., and Ryan, R. O. (1999) *J. Lipid Res.* **40**, 93–99
- Weisgraber, K. H., Lund-Katz, S., and Phillips, M. C. (1992) in *High Density Lipoproteins and Atherosclerosis* (Miller, N. E., and Tall, A. R., eds) Vol. III, pp. 175–181, Elsevier, Amsterdam
- Fisher, C. A., Narayanaswami, V., and Ryan, R. O. (2000) *J. Biol. Chem.* **275**, 33601–33606
- Raussens, V., Fisher, C. A., Goormaghtigh, E., Ryan, R. O., and Ruyschaert, J. M. (1998) *J. Biol. Chem.* **273**, 25825–25830
- De Pauw, M., Vanloo, B., Weisgraber, K., and Rosseneu, M. (1995) *Biochemistry* **34**, 10953–10966
- Lund-Katz, S., Zaiou, M., Wehrli, S., Dhanasekaran, P., Baldwin, F., Weisgraber, K. H., and Phillips, M. C. (2000) *J. Biol. Chem.* **275**, 34459–34464
- Westerlund, J. A., and Weisgraber, K. H. (1993) *J. Biol. Chem.* **268**, 15745–15750
- Dong, L. M., Wilson, C., Wardell, M. R., Simmons, T., Mahley, R. W., Weisgraber, K. H., and Agard, D. A. (1994) *J. Biol. Chem.* **269**, 22358–22365
- Fisher, C. A., Wang, J., Francis, G. A., Sykes, B. D., Kay, C. M., and Ryan, R. O. (1997) *Biochem. Cell Biol.* **75**, 45–53
- Morrow, J. A., Arnold, K. S., and Weisgraber, K. H. (1999) *Protein Expression Purif.* **16**, 224–230
- Vogel, T., Weisgraber, K. H., Zeevi, M. I., Ben Artzi, H., Levanon, A. Z., Rall, S. C., Jr., Innerarity, T. L., Hui, D. Y., Taylor, J. M., Kanner, D., Yavin, Z., Amit, B., Aviv, H., Gorecki, M., and Mahley, R. W. (1985) *Proc. Natl. Acad. Sci. U. S. A.* **82**, 8696–8700
- Maiorano, J. N., and Davidson, W. S. (2000) *J. Biol. Chem.* **275**, 17374–17380
- Davidson, W. S., Rodriguez, W. V., Lund-Katz, S., Johnson, W. J., Rothblat, G. H., and Phillips, M. C. (1995) *J. Biol. Chem.* **270**, 17106–17113
- Chattopadhyay, A., and London, E. (1987) *Biochemistry* **26**, 39–45
- Lund-Katz, S., Weisgraber, K. H., Mahley, R. W., and Phillips, M. C. (1993) *J. Biol. Chem.* **268**, 23008–23015
- Sparks, D. L., Phillips, M. C., and Lund-Katz, S. (1992) *J. Biol. Chem.* **267**, 25830–25838
- Narayanaswami, V., Szeto, S. S., and Ryan, R. O. (2001) *J. Biol. Chem.* **276**, 37853–37860
- Lowry, O. H., Rosenbrough, N. J., Farr, A. L., and Randall, R. J. (1951) *J. Biol. Chem.* **193**, 265–275
- Sokoloff, L., and Rothblat, G. H. (1974) *Proc. Soc. Exp. Biol. Med.* **146**, 1166–1172
- Narayanaswami, V., and Ryan, R. O. (2000) *Biochim. Biophys. Acta* **1483**, 15–36
- Innerarity, T. L., Friedlander, E. J., Rall, S. C., Jr., Weisgraber, K. H., and Mahley, R. W. (1983) *J. Biol. Chem.* **258**, 12341–12347
- Panagotopoulos, S. E., Horace, E. M., Maiorano, J. N., and Davidson, W. S. (2001) *J. Biol. Chem.*
- Ren, J., Lew, S., Wang, Z., and London, E. (1997) *Biochemistry* **36**, 10213–10220
- Abrams, F. S., and London, E. (1993) *Biochemistry* **32**, 10826–10831
- Baratti, J., and Maroux, S. (1976) *Biochim. Biophys. Acta* **452**, 488–496
- Lau, S. Y., Taneja, A. K., and Hodges, R. S. (1984) *J. Biol. Chem.* **259**, 13253–13261
- Frere, V., Sourgen, F., Monnot, M., Troalen, F., and Fermandjian, S. (1995) *J. Biol. Chem.* **270**, 17502–17507
- Segrest, J. P., Garber, D. W., Brouillette, C. G., Harvey, S. C., and Anantharamaiah, G. M. (1994) *Adv. Protein Chem.* **45**, 303–369
- Ladokhin, A. S. (1999) *Biophys. J.* **76**, 946–955
- Raussens, V., Slupsky, C. M., Sykes, B. D., and Ryan, R. O. (2003) *J. Biol. Chem.* **278**, 25998–26006
- Morrow, J. A., Arnold, K. S., Dong, J., Balestra, M. E., Innerarity, T. L., and Weisgraber, K. H. (2000) *J. Biol. Chem.* **275**, 2576–2580
- Weisgraber, K. H. (1990) *J. Lipid Res.* **31**, 1503–1511
- Saito, H., Dhanasekaran, P., Baldwin, F., Weisgraber, K. H., Lund-Katz, S., and Phillips, M. C. (2001) *J. Biol. Chem.* **276**, 40949–40954
- Dong, L. M., and Weisgraber, K. H. (1996) *J. Biol. Chem.* **271**, 19053–19057
- Saito, H., Dhanasekaran, P., Baldwin, F., Weisgraber, K. H., Phillips, M. C., and Lund-Katz, S. (2003) *J. Biol. Chem.* **278**, 40723–40729
- Choy, N., Raussens, V., and Narayanaswami, V. (2003) *J. Mol. Biol.* **334**, 527–539
- Yokoyama, S., Kawai, Y., Tajima, S., and Yamamoto, A. (1985) *J. Biol. Chem.* **260**, 16375–16382
- Small, D. M. (1986) in *The Physical Chemistry of Lipids: From Alkanes to Phospholipids*, pp. 175–520, Plenum Press, New York